

**WIRELESS ROGOWSKI COIL SENSOR BASED
ON PARTIAL DISCHARGE DETECTION SIGNAL
FOR ON-LINE CONDITION MONITORING IN
THE MEDIUM VOLTAGE POWER CABLES**

**MOHAMAD NUR KHAIRUL HAFIZI
BIN ROHANI**

**UNIVERSITI MALAYSIA PERLIS
2017**



**WIRELESS ROGOWSKI COIL SENSOR BASED
ON PARTIAL DISCHARGE DETECTION SIGNAL
FOR ON-LINE CONDITION MONITORING IN
THE MEDIUM VOLTAGE POWER CABLES**

by

**MOHAMAD NUR KHAIRUL HAFIZI BIN ROHANI
(1440911211)**

A thesis submitted in fulfillment of the requirements for the degree of
Doctor of Philosophy

**School of Electrical System Engineering
UNIVERSITI MALAYSIA PERLIS**

ACKNOWLEDGEMENTS

All thanks are to God for the opportunity and the strength He gave to complete this research. First and foremost to the superb mentor and would like to state his boundless appreciation to the superb mentor, my supervisors Assoc. Prof. Dr. Muzamir Isa, Dr. Baharuddin Ismail and Dr. Haziah Abdul Hamid, School of Electrical System Engineering, Universiti Malaysia Perlis (UniMAP) for their supervisions, continuous encouragement, inspiring suggestions and guidance throughout this research and preparation of this thesis.

I would like to extend my appreciation to my colleague Mr. Chai Chang Yii and Mr. Noor Syahril Noor Shah for their unbounded suggestion were helpful and shared important knowledge to bring out this to be success one. I would also like to extend my unlimited gratitude to all the partial discharge (PD) working group University Malaysia Perlis who rendered unfolded support for my research.

My outmost gratitude, I convey to my family especially my parent Hj. Rohani Bin Hj. Idris and Hjh. Aton Binti Hj. Mansor for their motivations and support along my research. Not forgetting my lovely wife Mrs. Afifah Shuhada Rosmi who had been a part of my carrier, your patience and sheer confidence in me made me the person I am now. She also has given birth our first child, Muhmmad Iman Iskandar on 2nd December 2016.

I would like also like to thank the Ministry of Higher Education of Malaysia for the sponsor of scholarship along the research study. I am also would like to thank School of Electrical System Engineering, Centre of Excellence for Advance Sensors Technology (CEASTech) and Centre of Excellence for Renewable Energy (CERE) for providing the experimental measurement facilities to accomplished my research. Last but not least, for all those whom I might not have mentioned here I seek sincere apology and thank everyone who had been a part of my success.

TABLE OF CONTENTS

	PAGE
DECLARATION OF THESIS	i
ACKNOWLEDGEMENTS	ii
LIST OF TABLES	vii
LIST OF FIGURES	ix
LIST OF ABBREVIATIONS	xiv
LIST OF SYMBOLS	xvi
ABSTRAK	xviii
ABSTRACT	xix
CHAPTER 1 INTRODUCTION	
1.1 Introduction	1
1.2 Research Problem Statement	3
1.3 Research Objective	5
1.4 Research Scope	5
1.5 Thesis Organization	7
CHAPTER 2 LITERATURE REVIEW	
2.1 Introduction	9
2.2 Partial Discharge Theory	9
2.3 Review on partial discharge Detection Methods	13
2.3.1 Optical Detection Method	13
2.3.2 Acoustic Detection Method	15

2.3.3	Chemical Detection Method	16
2.3.4	Chemical Detection Method	17
2.4	Rogowski Coil as a Partial Discharge Sensor	18
2.4.1	Rogowski Coil Sensor Design	19
2.4.2	Rogowski Coil Sensor Constructions	21
2.5	Electromagnetic Transient Program-Alternative Transient Program Software Environment	25
2.6	Partial Discharge Location Technique in Electromagnetic Transient Program-Alternative Transient Program Software Modelling	26
2.7	Filtering Technique by Implementing Active Filter	27
2.8	Overview on the Wireless Integration Approaches	28
2.9	Summary	29

CHAPTER 3 RESEARCH METHODOLOGY

3.1	Introduction	31
3.2	Rogowski Coil Sensor Development	34
3.2.1	Rogowski Coil Sensor Design	34
3.2.2	Rogowski Coil Sensor Characterization	37
3.2.3	Frequency Response Analysis	39
3.3	Electromagnetic Transient Program-Alternative Transient Program Modelling	40
3.3.1	Single-End Partial Discharge Measurement Technique	41
3.3.2	Comparison between Previous Research	42
3.3.3	Double-End Partial Discharge Measurement Technique	44
3.3.4	Comparison between Parameter of Three Core Unarmoured Copper Conductor 11 kV Cross-Linked Polyethylene Underground Power Cables	46

3.4	Partial Discharge Location Technique	46
3.4.1	Double-End Location Technique Implementation	46
3.4.2	Multi-End Partial Discharge Location Technique Implementation	47
3.5	Experimental Measurement Setup	
3.5.1	Effect of Shielded Rogowski Coil Sensor for Partial Discharge Measurement	53
3.5.2	Effect of Terminating Resistance, R_t	54
3.6	Clamp Rogowski Coil Sensor Design and Implementation	54
3.7	Non-Inverting Operational Amplifier and Active Filter Implementation	55
3.8	Wireless Rogowski Coil Sensor Integration	59
3.8.1	Sigma-Delta Analog to Digital Converter Topology Implementation	61
3.8.2	Partial Discharge Detection Method	64
3.8.3	Transceiver Module	65
3.9	Device Setup	66
3.9.1	SignalTap II Logic Analyser	67
3.9.2	Altera DE0-Nano Development Board	68
3.9.3	Altera DE2-115 Development Board	69
3.10	Summary	70

CHAPTER 4 RESULTS AND DISCUSSION

4.1	Introduction	71
4.2	Rogowski Coil Sensor Characterizations Result	72
4.2.1	Frequency Response Evaluation Results	73
4.3	Electromagnetic Transient Program-Alternative Transient Program Simulation Results	75

4.3.1	Single-End Simulation Result with Different Type of Rogowski Coil Sensor	75
4.3.2	Simulation Results in Comparison between the Previous Designs of Rogowski Coil Sensors	79
4.3.3	Double-End Technique Simulation Results with Different Size of Nominal Area Conductor Cable	80
4.4	Partial Discharge Location Technique Simulation Results	83
4.5	Rogowski Coil Experimental Results	84
4.5.1	Experimental Results for Different Type of Rogowski Coil Sensors	85
4.5.2	Effect of Shielded Rogowski Coil Sensor for Partial Discharge Measurement Results	88
4.5.3	Effect of Terminating Resistance, R_t Results	91
4.6	Active Filter Implementation	92
4.7	Wireless Rogowski Coil Sensor Integration Result	95
4.8	Summary	99
 CHAPTER 5 CONCLUSIONS		
5.1	Conclusion	101
5.2	Research Findings	102
5.3	Recommendation and Future Work	104
 REFERENCES		106
 LIST OF PUBLICATIONS		112
 LIST OF AWARDS		114
 APPENDIXES		115

LIST OF TABLES

NO.		PAGE
2.1	Comparison between existing current sensors characteristic (Xiao et al., 2003).	17
2.2	Shielding efficiency of RC sensor (Hlavacek et al., 2016).	24
3.1	Design parameter of <i>RC 1</i> , <i>RC 2</i> , <i>RC 3</i> and <i>RC 4</i> sensor	37
3.2	Geometrical of RC sensor parameters.	43
3.3	RC sensor model parameters.	44
3.4	Three-core XLPE 11 kV unarmoured cable parameters.	46
3.5	Dimension parameter of shell design.	53
3.6	List of second order active high pass Butterworth filter (Sallen-key topology) components.	57
3.7	List of RF module specifications.	66
3.8	Altera DE0-Nano and DE2-115 FPGA board comparison.	67
4.1	Characterization Parameter of PD sensor.	72
4.2	Simulation results for frequency response analysis summary.	74
4.3	Simulation results for <i>RC 1</i> , <i>RC 2</i> , <i>RC 3</i> and <i>RC 4</i> summary.	78
4.4	Summary of simulation results for RC sensor.	80
4.5	PD data analysis measured by RC sensor using double-end technique.	83
4.6	PD data analysis measured by RC sensor using multi-end technique.	85
4.7	Experimental result for <i>RC 1</i> , <i>RC 2</i> , <i>RC 3</i> and <i>RC 4</i> .	88
4.8	Measurement results by unshielded and shielded RC for the injected 1 V up to 5 V PD pulse amplitude.	91
4.9	Calculated value for sampling time and sampling number in 1 μ s PD signal.	96

©This item is protected by original copyright

LIST OF FIGURES

NO.		PAGE
1.1	Percentage of unscheduled supply interruption by type of interruptions (Energy Commission of Malaysia, 2015).	2
1.2	Leaning rubber tree on the 33 kV overhead power cables at Felda Chuping, Perlis, Malaysia.	3
2.1	Type of partial discharge, (a) internal discharge, (b) corona discharge, (c) surface discharge, and (d) discharge by electrical treeing (Boonruang and Suphachai, 2011).	11
2.2	PD analysis in frequency domain for different XPLE power cable defect, (a) stress cone dislocation, (b) insulation scratches, (c) external damage, and (d) floating aluminium sheath (Xu et al., 2016).	12
2.3	PD detection method for power components (Li, Xutao, Liu, and Yao, 2016 and Mohammadi and Haghjoo, 2016, 2017).	13
2.4	Schematic drawing of the test setup of F-POF assisted optical coincidence PD measurement (Siebler et al., 2015).	14
2.5	PD measurement system using optical transmission (Tian et al., 2004).	15
2.6	Experimental setup by using an AE sensor placed on the jointing XLPE cable (Wang et al., 2007).	16
2.7	PD sensor. (a) RC sensor working principal, (b) RC sensor equivalent circuit (Isa et al., 2012).	19
2.8	RC sensor constructed using a plastic pipe with a hollow inner for return wire (Shafiq et al., 2014).	22
2.9	Frequency response of shielded and unshielded RC sensor (Hemmati and Shahrtash, 2012).	24
2.10	Schematic of three phase PD monitoring system for CC overhead lines (Isa et al., 2009).	26
2.11	EMTP-ATP modelling on three phase PD monitoring system for CC overhead lines (Isa et al., 2009).	27
2.12	The non-inverting active low pass integrator, (a) equivalent circuit of the non-inverting active low pass integrator and (b) the constructed non-inverting active low pass filter (Yutthagowith, 2016).	28

3.1	Process flow of the prototype development.	33
3.2	Different cross-section of RC sensor, (a) Circular, (b) Square and rectangular and (c) Oval.	35
3.3	Prototype modeling using SolidWorks 3D CAD software and printed version, (a) circular shape (<i>RC 1</i>), (b) Square shape (<i>RC 2</i>), (c) Rectangular shape (<i>RC 3</i>) and (d) oval shape (<i>RC 4</i>).	36
3.4	Equivalent circuit for capacitance value measurement of RC sensor.	38
3.5	Lumped parameter of the RC sensor model using PSIM software.	40
3.6	Single-end line diagram of off-line monitoring system with PD effect on the MV cable.	42
3.7	Simulated 5nC calibrator pulses (Hashmi, 2008 and Isa, 2013).	42
3.8	Single-end PD measurement technique with sensor modeling using EMTP-ATP tools software.	43
3.9	Double-end line diagram of off-line monitoring system with PD effect on the MV underground cable.	44
3.10	Double-end PD measurement technique with RC sensor modeling using EMTP-ATP tools software.	45
3.11	Multi-end PD location technique, (a) PD occur between point A and B, and (b) PD occur at point B and C.	47
3.12	Multi-end PD location technique in ATPDraw, (a) PD injected between A and B, and (b) PD injected between point B and C.	49
3.13	Research tools and equipment.	50
3.14	Schematic diagram for experimental setup.	51
3.15	Generated PD pulse using Agilent Benchlink Waveform Builder tools software.	52
3.16	Continuous 1 MHz PD signals generated by Agilent 81150A Pulse Function Arbitrary Generator.	52
3.17	Prototype of RC sensor, (a) unshielded RC sensor, and (b) shielded RC sensor RC sensor clamp on the copper rod.	53
3.18	RC sensor position with clamp on the 240 mm ² nominal area for 11 kV XLPE underground power cable, (a) unlock RC sensor, and (b) locked RC sensor.	55

3.19	Illustration of second order filter.	56
3.20	Second order active high pass Butterworth filter (Sallen-key topology).	56
3.21	Schematic circuit of non-inverting operational amplifier and active Butterworth high-pass filter using OrCAD software.	58
3.22	Non-inverting op- amp and active Butterworth high-pass filter circuit fabrication.	58
3.23	Diagram of wireless RC sensor for on-line PD monitoring system on MV power cable.	59
3.24	Wireless integration for PD detection technique.	60
3.25	Experimental configuration for PD measurement in the laboratory.	60
3.26	Implementation of $\Sigma\Delta$ ADC in FPGA.	63
3.27	Peak detector and thresholding technique.	64
3.28	Process flow for PD detection method.	65
3.29	RF module S14463.	66
3.30	SignalTap II analyser configuration.	67
3.31	Pin assignment using pin planner in Quartus II software.	68
3.32	Hardware measurement setup for transmitter part.	69
3.33	Hardware measurement setup for receiver part.	69
4.1	Bode plots for measured lumped parameter model of RC 1.	73
4.2	Bode plots for measured lumped parameter model of RC 2.	73
4.3	Bode plots for measured lumped parameter model of RC 3.	74
4.4	Bode plots for measured lumped parameter model of RC 4.	74
4.5	Current PD pulse at distance of 5 km at Phase A, B and C.	76
4.6	Simulation result in distance of 5 km from PD source, (a) in the time and (b) frequency domain for RC 1.	77
4.7	Simulation result in distance of 5 km from PD source, (a) in the time and (b) frequency domain for RC 2.	77

4.8	Simulation result in distance of 5 km from PD source, (a) in the time and (b) frequency domain for <i>RC 3</i> .	78
4.9	Simulation result in distance of 5 km from PD source, (a) in the time and (b) frequency domain for <i>RC 4</i> .	78
4.10	Simulation result at phase A, B and C, (a) <i>RC sensor A</i> and (b) <i>RC sensor B</i> , in time domain.	80
4.11	Simulation result at phase A with <i>RC sensor A</i> , <i>B</i> , and <i>RC 3</i> in frequency domain.	80
4.12	Simulation result for different nominal size XLPE conductor cable.	81
4.13	The arrival time for different size XLPE nominal size conductor cable.	82
4.14	The propagation velocity with different nominal size XLPE conductor cable.	82
4.15	Double-end PD simulation result at point A and point B.	83
4.16	Multi-end PD simulation results at point A, B and C	84
4.17	PD sensor's response for the injected 1 MHz pulse calibrator, (a), (b), (c), (d) in the time domain for <i>RC 1</i> , <i>RC 2</i> , <i>RC 3</i> and <i>RC 4</i> respectively.	87
4.18	PD sensor's response for the injected 1 MHz pulse calibrator, (a), (b), (c), and (d) in the frequency domain for <i>RC 1</i> , <i>RC 2</i> , <i>RC 3</i> and <i>RC 4</i> respectively.	88
4.19	PD sensors with unshielded and shielded response for the injected 5 V PD pulse amplitude in time domain, (a) unshielded and (b) shielded.	89
4.20	PD sensors with unshielded and shielded response for the injected 5 V PD pulse amplitude in frequency domain (a) unshielded and (b) shielded.	90
4.21	Effect of terminating impedance for unshielded and shielded RC sensor on the performance of PD measurements in time domain.	92
4.22	Effect of terminating impedance for unshielded and shielded RC sensor on the performance of PD measurements in frequency domain.	92
4.23	Frequency response analysis for non-inverting operational amplifier and active high-pass Butterworth filter using Sallen-key topology.	93

4.24	Amplify and filtering implementation on RC sensor output results for PD measurement.	94
4.25	Notification at Altera DE2-115 as a receiver unit, (a) good condition and no PD signal detected and (b) PD signal is detected.	95
4.26	4-bit resolutions sampling signal for PD measurement using $\Sigma\Delta$ ADC topology in SignalTap II analyser.	97
4.27	5-bit resolutions sampling signal for PD measurement using $\Sigma\Delta$ ADC topology in SignalTap II analyser.	98
4.28	6-bit resolutions sampling signal for PD measurement using $\Sigma\Delta$ ADC topology in SignalTap II analyser.	98
4.29	7-bit resolutions sampling signal for PD measurement using $\Sigma\Delta$ ADC topology in SignalTap II analyser.	98
4.30	8-bit resolutions sampling signal for PD measurement using $\Sigma\Delta$ ADC topology in SignalTap II analyser.	99

©This item is protected by original copyright

LIST OF ABBREVIATIONS

3D	3 Dimension
ABS	Acrylonitrile Butadiene Styrene
AC	Alternating Current
ADC	Analog to Digital Converter
CAD	Computer Aided Design
CC	Capacitive Coupler
DGA	Dissolved Gas Analysis
DSI	Discrete Spectral Interference
EMI	Electromagnetic Interference
EMTP-ATP	Electromagnetic Transient Program-Alternative Transient Program
FEM	Finite Element Method
FPGA	Field-Programmable Gate Array
F-POF	Fluorescent Polymer Optical Fiber
GMR	Giant Magneto Resistive
HE	Hall Effect
HFCT	High Frequency Current Transformer
HV	High Voltage
IoT	Internet of Thing
LCC	Line Communicate Converter
MI	Magneto Impedance
MV	Medium Voltage
PD	Partial Discharge
PLA	Polylactic Acid

PMT	Photon Multiplier Tubes
PSIM	PowerSim
RC	Rogowski Coil
RF	Radio Frequency
RMS	Root Mean Squares
SMD	Surface Mount Device
VHDL	Verilog Hardware Description Language
XLPE	Cross-Linked Polyethylene

©This item is protected by original copyright

LIST OF SYMBOLS

C_{gap}	Gap Capacitance
C_l	Lumped Capacitance
D_{rc}	Diameter Rogowski Coil Sensor
D_{wire}	Diameter Wire
L_l	Lumped Inductance
M_c	Coil Mutual Inductance
R_{in}	Inner Radius
R_l	Lumped Resistance
R_{out}	Outer Radius
V_{out}	Output Voltage
V_p	Peak Value
V_{pp}	Peak to Peak Voltage
V_{rc}	Rogowski Coil Output Voltage
Z_{out}	Terminating Impedance
f_r	Resonant Frequency
t_d	Time Different of Arrival Time
$\Sigma\Delta$	Sigma-Delta
A	Area
B	Magnetic Density
g	Turn to Turn Distance
h	Height
l	Length of wire
L	Total length of the cable

N	Number of Turns
λ	Flux Linkage
Ω	Resistance (ohm)
X	Location of PD pulse
v	Propagation velocity
ρ	Copper Resistivity

©This item is protected by original copyright

Penderia Gegelung Rogowski Tanpa Wayar untuk Pengesanan Isyarat Pelepasan Separa Pada Keadaan Pemantauan Atas Talian Dalam Kabel Voltan Sederhana

ABSTRAK

Pengukuran pelepasan separa (PD) menyediakan maklumat yang berharga untuk menilai keadaan penebat voltan tinggi (HV) pada sistem kuasa. Dalam kajian ini, penderia gegelung Rogowski (RC) tanpa wayar yang baharu berdasarkan kepada pengesanan PD dalam kabel kuasa voltan sederhana (MV) dibentangkan. Kajian ini dibahagikan kepada tiga bahagian iaitu pembangunan penderia PD, teknik pra-penapisan dan integrasi tanpa wayar. Satu siri siasatan ke atas kepekaan dan jalur lebar untuk empat jenis penderia RC ditunjukkan. Pembangunan prototaip pertama telah dijalankan dengan bantuan perisian SolidWorks 3-dimensi (3D) bantuan komputer reka bentuk (CAD) dan pencetak MakerBot 2X 3D. Selepas itu, penderia dimodelkan dan simulasi menggunakan perisian *Electromagnetic Transient Program-Alternative Transient Program* (EMTP-ATP) berdasarkan parameter yang telah dikenalpasti. Satu teknik pengukuran penamatan tunggal (*single-end*) telah digunakan sebagai sistem pemantauan PD dalam talian pada tiga fasa voltan sederhana *cross-link polyethylene* (XLPE) kabel kuasa bawah tanah dengan keluasan 240 mm² konduktor tembaga. Untuk mengesahkan keputusan yang dicapai dari simulasi, pengukuran eksperimen telah dijalankan. Eksperimen ini telah diulang bagi setiap reka bentuk penderia RC. Dalam usaha untuk mencapai penderia PD yang terbaik, pilihan yang tepat adalah paling utama. Dalam kes ini, keputusan menunjukkan bahawa bentuk geometri segi empat tepat mempunyai prestasi yang lebih baik merujuk kepada pengesanan isyarat PD. Bentuk segi empat tepat penderia RC telah dipilih untuk dibandingkan dengan penderia konvensional RC yang lain. Teknik pengukuran dua penamatan (*double-end*) telah digunakan di mana dua daripada penderia RC diletakkan pada jarak tertentu untuk menganalisis halaju perambatan dan masa ketibaan isyarat PD ditangkap oleh penderia berdasarkan saiz XPLE kabel kuasa yang berbeza. Analisis ke atas ketepatan teknik lokasi *double-end* dan *multi-end* PD telah dijalankan. Keputusan teknik lokasi *double-end* dan pelbagai penamatan (*multi-end*) PD masing-masing mempunyai 0.138 % dan 0.026 % peratusan ralat. Satu eksperimen telah dijalankan untuk menilai kesan perbezaan penderia RC tidak terlindungi, dilindungi dan perintang penamatan, R_t . R_t adalah sebahagian daripada parameter yang boleh meningkatkan prestasi penderia RC. Penguat kendalian (*op-amp*) dan penapis *Butterworth* laluan tinggi aktif yang telah direka dengan menggunakan topologi *Sallen-key* yang digunakan untuk menguatkan dan menyekat gangguan isyarat keluaran daripada penderia RC dalam bahagian kedua. Integrasi penderia RC ke dalam sistem komunikasi tanpa wayar telah dibincangkan dalam bahagian akhir. Peranti penukar analog kepada digital (ADC) berkelajuan tinggi diperlukan untuk menyempel isyarat PD. Walau bagaimanapun, ADC konvensional di pasaran adalah lebih mahal untuk kelajuan yang tinggi. Oleh itu, Sigma-Delta ($\Sigma\Delta$) ADC topologi dibangunkan dalam Altera DE0-Nano. Pengesanan puncak dengan teknik had diperkenalkan dalam bahagian ini. Kemudian, data yang akan dihantar secara tanpa wayar kepada unit pengkalan menggunakan modul frekuensi radio (RF) sebagai *transceiver* dan Altera DE2-115 digunakan sebagai unit pengkalan. Dalam usaha untuk mencapai persampelan digital yang tepat frekuensi tinggi isyarat PD, N-bit resolusi adalah paling utama. Dapatan analisis ini, resolusi 4-bit dipilih dalam kajian ini sebagai penyelesaian yang terbaik untuk $\Sigma\Delta$ ADC untuk persampelan isyarat PD.

Wireless Rogowski Coil Sensor Based On Partial Discharge Detection Signal for On-Line Condition Monitoring in the Medium Voltage Power Cables

ABSTRACT

Partial discharge (PD) measurement provide a valuable information for assessing the insulation health in high voltage (HV) power system. In this research, a novel wireless Rogowski coil (RC) sensor based on PD detection in the medium voltage (MV) power cables is presented. This research is divided into three sections which are RC sensor development, pre-filtering technique and wireless integration. A series of investigations on sensitivity and bandwidth for four types of RC sensors was demonstrated. The prototype development first was carried out with the assistance of SolidWorks 3 dimension (3D) computer aided design (CAD) software and MakerBot 2X 3D printer. Subsequently, the sensors were modeled and simulated using Electromagnetic Transient Program-Alternative Transient Program (EMTP-ATP) software environment based on the lumped parameter identification. A single-end measuring technique was used as an on-line PD monitoring system on the three-phase medium voltage underground cross-link polyethylene (XLPE) insulated power cable with a 240 mm² nominal area copper conductor. In order to verify the simulation results, an experimental measurement was carried out. This experiment was repeated concurrently for each design of the RC sensors and the precise selection for the best sensor is paramount. In this case, the results indicated that rectangular geometrical shape performed better with regard to the detection of the PD signal. The rectangular shapes of RC sensor has been selected in order to compare with the conventional RC sensor. Double-end technique measurement has been used where two of RC sensor is placed on the certain distance to analyse the propagation velocity and arrival time of PD signal captured by the sensor based on the different size of XPLE power cables. The analysis on accuracy of double-end and multi-end PD location technique have been conducted. The results between double-end and multi-end technique have 0.138 % and 0.026 % percentage error of PD location respectively. An experiment has been conducted in order to evaluate the effect of unshielded, shielded RC sensor and terminating resistance, R_t . The R_t is a part of parameter which can improve the performance of RC sensor. An operational amplifier (op-amp) and active Butterworth high-pass filter which has been designed using Sallen-key topology that is used to amplify and suppress the noise of output signal from RC sensor in the second section. The integration of RC sensor into wireless communication system has been discussed in the final section. High speed analog to digital converter (ADC) device is required to sample the PD signal due. However, the conventional ADC in the market is expensive in high speed rate. Thus, Sigma-Delta ($\Sigma\Delta$) ADC topology is developed in Altera DE0-Nano board. Peak detection with threshold technique is introduced in this section. Then, the data transmitted wirelessly to the server unit using radio frequency (RF) module as a transceiver and Altera DE2-115 board is used as a server unit. In order to achieve the accurate digital sampling of high frequency PD signal, the N-bit resolution is paramount. The finding of this analysis, 4-bit resolution is selected in this research as the best resolution for the $\Sigma\Delta$ ADC to sampling the PD signal.

CHAPTER 1

INTRODUCTION

1.1 Introduction

Recently, electrical utility companies are enhancing their focus on the modernization of their distribution systems. The upgrading exercise is aimed to improve on reliability, efficiency and safety of the system. The utmost issue when discussing on the issue of reliability is an unscheduled interruption due to faulty electrical equipment. In Peninsular Malaysia, the annually energy demand increased 2.22 % from 112,358 in 2013 to 114,856 GWh in 2014 was recorded (Energy Commission of Malaysia, 2015). However, the disruption from power system fault will lose in a million of Ringgit Malaysia. Based on the percentage of unscheduled interruption recorded by NUR Distribution Sdn. Bhd. as a one of electricity distribution company in Malaysia as shown in Figure 1.1, the faulty equipment contributes the highest percentage which is 51.91 % and followed by overload, 23.08 %, damage by third party and quality of material are 9.62 %. Lastly, natural disasters such as wind, storm, flood, landslide and others are 5.77 %. As the energy supplier, the percentage of the unscheduled interruption should be as low as possible. The earlier interruption detection in the power system via modern technologies is necessary.

It was reported that insulation failure is mostly caused by electrical equipment's fault (Williams et al., 2002, and Raymond et al., 2015). Part of the statistic is contributed by a breakdown in power cables. Medium voltage (MV) cross-linked polyethylene

(XLPE) underground power cables are widely used in the power distribution, especially in the urban area. Distribution power line using XLPE power cables have become widely used because of their advantages such as lightweight structure, easy to bend, excellent electrical properties, heat resistance, transmission capacity and easy installation (Hu and Duan, 2015).

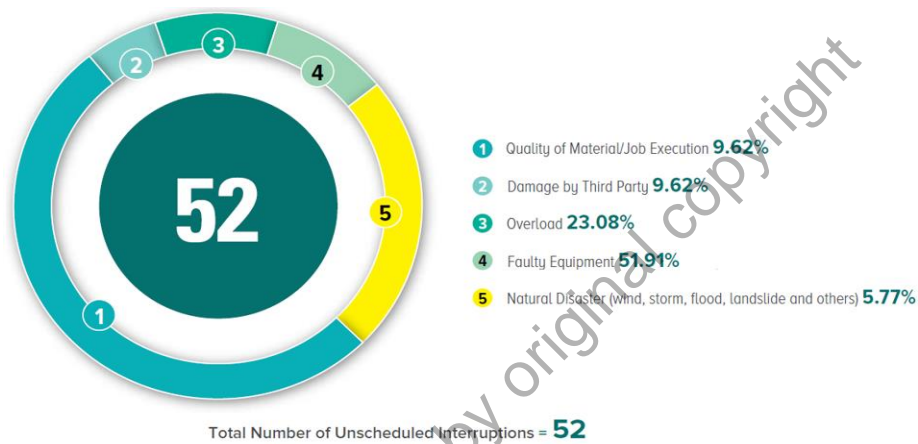


Figure 1.1: Percentage of unscheduled supply interruption by type of interruptions (Energy Commission of Malaysia, 2015).

However, partial discharge (PD) phenomenon may lead towards insulation degradation in high voltage (HV) power cables. PD is a symptom before the fault happened (Sarathi and Raju, 2005, El Mountassir, Stewart, Reid, and McMeekin, 2017, and Ibrahim and Abd-Elhady, 2017). Figure 1.2 shows the scenario of leaning rubber tree on the 33 kV XLPE power cables at Felda Chuping, Perlis, Malaysia. The falling rubber tree on the XLPE power cables may cause PDs activity which can be treated as a gliding discharge due to electric field around the cables is heavily distorted (Hashmi, 2008). PDs are produced in the air gap between the surface of the rubber tree and XLPE cables insulation. This condition may eventually cause to a total failure and in the meantime considerably reduce the life span of the power cable. Therefore, the early stage of fault detection in a power system is required in order to ensure that the MV XLPE power cables

are in a good condition. Higher sensitivity and wider bandwidth sensors as an indication of insulation's health are necessary in detecting the PD signal as well.



Figure 1.2: Leaning rubber tree on the 33 kV overhead power cables at Felda Chuping, Perlis, Malaysia.

1.2 Research Problem Statement

Currently, the conventional sensors which has low detection in terms of sensitivity and bandwidth is a major concern in early stage of PD monitoring on HV insulation material (Olmos, Primicia, and Marron, 2007). PD sensor for insulation monitoring must be installed in on-line condition on power distribution network (Zhou, Han, and Qing, 2014). Several sensor can be installed during operation such as high frequency current transformer (HFCT) without switch off the power grid and may not risk of failure for the power lines (Sheng, Zhou, Hepburn and Dong, 2015, and Álvarez, Garnacho, Ortego, and

Sánchez-Urán, 2015). However, the limitation in term of saturation, size, weight and high cost if frequently used. The non-conventional sensor such as RC sensor has increased popularity in PD monitoring system. The selection of RC sensor as a PD sensor in this research is based on the characteristic such as wide bandwidth, lightweight, linearity, fast response, no hysteresis losses, low cost and easy to construct in the laboratory (Wang, Yuan, Wang, and Liu, 2011). However, the RC sensor has low sensitivity bandwidth and robustness due to the air-cored inductive sensor. In addition, the limitation to fabricate the core material as a support of RC winding wire due to accurate shape and geometry was addressed.

Then, the noisy background is influenced during the on-line PD measurement by using the inductive sensor for the insulation monitoring (Zhang, Blackburn, Phung, and Sen, 2007, Seo, Ma, and Saha, 2015, and Montanari, 2016). By reducing the noise background that distort the pure PD signal makes it easier to be detected.

Traditionally, the on-line PD measurement is not practically and economically been possible. The high cost of equipment and specialist are needed during the measurement process (Hashmi, Lehtonen, and Mikael Nordman, 2010, and Nimsanong, Pattanadech, and Yutthagowith, 2016). The data measurement is collected manually for every sensor on the power lines needs the time consumption and labor force. Thus, a design of wireless sensor for PD detection signal on the medium voltage (MV) XLPE underground power cables is a novel for this research. The RC sensor is selected according to the superior characteristics compared to the conventional PD sensor and matching with the requirement of this system.